

Improvement of small scale mine blast operation: a comparative application of hunter-point artificial neural network, support vector machine, and regression analysis models

B.O. Taiwo ^{a,*}, A.I. Ajibona ^a, K. Idowu ^b, A. S. Babatunde ^c, O.B. Ogunyemi ^a

^a Federal University of Technology Akure, Mining Engineering, Nigeria.

^b University of Jos, Mining Engineering, Nigeria.

^c School Mines, China University of Mining and Technology, Xuzhou China.

Article History:

Received: 04 August 2022.

Revised: 27 December 2022.

Accepted: 24 February 2023.

ABSTRACT

The blasting operation is one of the technologies used for breaking rock masses and reducing the rock mass into smaller sizes to improve transportation and further particle separation. The improvement of blast fragmentation supports the maximization of mining operation and productivity. Soft computing and regression model has been developed in this study to optimize small-scale dolomite blast operations in Akoko Edo, Nigeria. WipFrag software was used to analyze the results of 35 blasting rounds. As independent variables, one uncontrollable parameter and five controllable blast parameters were chosen to predict blast particle sizes using four mathematically motivated soft computing model approaches. The prediction accuracy of the developed models was tested using various model performance indices. The study revealed that rock strength influences blast fragmentation results, and based on the rock strength properties, the fragmentation block size increases with an increase in rock strength. The results of the model performance indices used for the evaluation of the proposed models showed that the modified Artificial Neural Network (ANN) called Hunter Point (HP-ANN) has the highest predictive accuracy. A new model evaluator was also developed in this study called the decision factor. Its application indicates that the HP-ANN model is the best model suitable for the prediction of blast fragment size distribution. Therefore, the developed models can be used to predict the blast result mean size (X_{50}) and the 80% percentage passing size (X_{80}) for mining engineering blasting practices.

Keywords: Artificial neural network, Blasting, Empirical modelling, Support vector machine, WipFrag software.

1. Introduction

The reduction of rock size using explosives materials is performed in mines to reduce in-situ rock mass into smaller particle sizes that can be easily handled by loading and haulage equipment. The improvement of small-scale blasting will directly assist the mine management to minimize operational costs and optimize productivity in the mine. Explosives are energetic materials widely used for rock mass fragmentation in mining and civil engineering operations [1]. The rock blasting operation could be referred to as the first comminution process in quarrying and mining, and as a result of this, the size of fragments obtained should not exceed the gape of the downstream primary crusher for efficient beneficiation [2-3]. The rock mass blasting process involves breaking massive rock formations to extract the largest possible size at a reduced cost. To achieve this objective, control of explosive-induced energy is an essential condition that must be satisfied to avoid poor blast results and environmental damages [4-5]. The main target of mine blasting design is to guarantee productive and environmentally friendly fragmentation under existing working conditions [6]. Taiwo revealed that blasting fragmentation size distribution is influenced by uncontrollable factors and the explosive charge proportion [7]. The blast Controllable factors are parameters under the control of the blast engineer; which can be easily changed to adjust the blasting result. Title explained that the uncontrollable factors are constrained by the rock's

discontinuity nature, heterogeneity, anisotropy, and non-elastic properties [8]. The prediction and assessment of the rock size distribution during the blasting operation is important to understand the blasting result efficiency [9]. In mining operations, the distribution of rock blast fragmentation has a high influence on the rate of productivity and downstream operational efficiency [10]. As indicated by Thurley [11], there are many fragmentation measurement methods used for assessing the results of blasting operations. Among these methods are, the oversize boulder count, sieving, visual analysis, shovel loading rate, and image analysis [12]. The artificial neural network has been found important in research works and the development of prediction models in the mining engineering field according to Abiodun et al. [13]. Various conventional statistical methods, empirical equations, and artificial neural network systems have been utilized by different researchers to predict rock fragment size distribution and other impacts of blasting operations [14-17].

Rezaei et al. [18] used the Multi-Layer Perception type of feed-forward back-propagation neural network with an architecture of 9-5-5-1 to develop a new predictive model for estimating the height of the distressed zone (HDZ), and the results were compared with conventional regression analysis (CRA). The comparative analysis performed between the proposed models and available models for

* Corresponding author. E-mail address: taiwoblessing199@gmail.com (B.O. Taiwo).

predicting the height of the distressed zone demonstrates that the results of the ANN model are consistent with the results of previous models, particularly in-situ measurements and empirical models. The ANN model also takes into consideration the possible effective parameters on the HDZ. In an iron ore mine, Bahrami et al. [16] used the artificial neural network (ANN) method to develop a prediction model for rock fragmentation induced by blasting. Their findings were discussed using eight parameters as input variables: hole diameter, burden, powder factor, and blastability index. The study demonstrates that the ANN technique is an effective method for predicting and improving blast fragmentation. The study was unable to compare the performance of the developed model to that of other Artificial Intelligence (AI) techniques and was primarily concerned with large-diameter iron ore mining operations. Sayadi et al. [17] used various ANN models to predict simultaneous rock fragmentation and back break in the blasting operation of Tehran Cement Company limestone mines in Iran. Through an empirical and soft computing modelling approach, the study also revealed ANN as a supportive approach for improving blasting operations. Nonetheless, the work focuses on large-diameter drill hole blasting, leaving unanswered the question of ANN performance with small-diameter drill holes. Amoako et al. [20] also use ANN and hybrid support vector machine learning to predict blast fragmentation. Therefore (AI) approaches are preferred over other predictive modelling methods because of their capacity to incorporate various variables influencing the result of a blast among different benefits as revealed by Rezaei et al. [18], and Amoako et al [20].

This paper adopted ANN, SVM, Ridge, and Multivariate (MVR) regression models for the development of blast particle size distribution prediction models. Several previous papers had focused on developing mean fragment size prediction models for large-scale blast operation; this paper attempts to minimize the loss in production and costly trial and error blast design in dolomite quarries through the development of optimum prediction models using combined soft computing and regression analysis approaches. The blast design parameters and rock strength property of thirty-five blasting operations were gathered and utilized as the input parameters to develop the proposed models. ANN, SVM, Ridge regression, and multivariate regression were used to develop the proposed models. The accuracy of the established models was tested using various prediction performance indices. The study also proposes a new prediction performance index to determine the accuracy of the models' forecasting.

2. Review of blast operation prediction attempts

Blasting is an art, and the professionalism and technical expertise of the blaster, play an important role to ensure productive and safe results [21]. Several authors have explored the improvement of blasting operations through adjustments in blast controllable parameters, empirical modifications, and comparisons. These authors have adopted various blast controllable parameters, and it was discovered that none of the developed formulae took into account all properties and conditions available due to the heterogeneity of the blasting operation and rock formation.

Da Gama proposed a microcomputer simulation model and a Communion Theory model for predicting blast results using selected parameters [22-23]. Babaeian et al. [24] identified the main disadvantage of the model as the fact that the effect of stemming length, spacing, and bench height was ignored, as well as the absence of non-uniformity and uniformity prediction factors. Larsson et al. and Kuznetsov's models were introduced in the 1970s as predicting formulas to improve blasting efficiency by predicting possible fragmentation results from specific combinations of blast parameters [25-26]. The models took into account factors, such as explosive type, rock mass classification, the impact of applied blast energy, and the evaluation of fragmentation uniformity and non-uniformity. The models' prediction performance was criticized due to their poor performance in predicting particle size distribution [24]. In 1983, the emergence of the Kuz-Ram model by Cunningham [27] came to the industry phase as a way to

improve blasting work and cover up for previous models with limitations in applicability and efficiency. limitations. The model proposed an empirical equation (Eq. 1) for predicting the 50% passing size of a blasting round, considering both controllable and uncontrollable parameters that influence the rock fragmentation result. The first version of the model was further improved by Cunningham through the adoption of the Lilly blastability index to properly assess the model's performance and account for rock site condition and specification [27-30].

$$X_{50} = Aq^{0.8} \times Q^{1/6} \left(\frac{115}{S_{ANFO}} \right)^{19/30} \quad (1)$$

Where Q is the mass of explosives utilized in kg, A is the rock factor, q denotes the powder factor in kg/m³, A is the rock factor, and S_{ANFO} represents the relative effective energy of the explosive. Cunningham also developed the Kuznetsov-Cunningham-Ouchterlony (KCO) fragmentation model in 2005 as an extension of the Kuz-Ram model [31]. The Swebrec function was added to the Kuz-Ram model by the KCO model, replacing the Rosin-Rammler equation. The KCO model (Eq. 2) was proposed to help minimize the two limitations of the Kuz-Ram model: poor prediction ability for fine fragments and poor estimation of the upper limit size range of fragmentation block sizes [31]. Singhai and Pyasi demonstrated that networks of artificial neurons could be used to compute arithmetic or logical functions [32]. Their work has been recognized as the origin of the application of ANN techniques since 1940. Furthermore, many prediction models, including [13-16, 20, 33-34] have been developed to determine the performance of blasting operations using an AI approach and proposed computing equations.

$$X_{50} = Aq^{0.8} \times Q^{1/6} \left(\frac{115}{S_{ANFO}} \right)^{19/30} \quad (2)$$

3. Materials and Methods

3.1. Description of the study area

The study area is located in the Akoko Edo Local Government, Edo State, Nigeria. The quarry produces dolomite boulders and is currently in operation.

Figures 1 and 2 show the Geological Map of the Golden Girl quarry in Akoko Edo, Edo State as extracted from the Geological Map of Nigeria, and the mine site, respectively. The Golden Girl quarry is located in Ikpeshi, Akoko Edo, Edo State, lying within latitudes 7°08'N to 7°10'N and longitudes 6°10'E to 6°15'E and forming part of the Igarra schist belt.

3.2. Methodology used in data analysis

Fragmentation analysis is an approach used to evaluate the rate of rock disintegration or particle size reduction after a blasting operation. For the quantification, size estimation, and distribution of fragmented rocks, can be obtained by taking sample images of a muck pile, truck, or conveyer belt [35]. Rock fragmentation during mining operations begins with the drilling and blasting process [8].

In conducting this research, blasting data relating to different blasting parameters were collected to cover a wide range of values for the burden-to-spacing ratio, stiffness ratio, drill hole diameter-to-burden ratio, stemming length, and powder factor. In the case study quarry, thirty-five scaled blast images were captured from different pit locations after each blast round. The images were analyzed separately using WipFrag 3.3[©] software. Drilling is carried out in the Golden Girl dolomite quarry by a Jackhammer and pneumatic compressor. The blast hole diameter of 40 mm is drilled vertically with staggered and square drill-hole patterns to different depths ranging from 1.4 m – 1.45 m. Explosive charging is administered using non-electric (NONEL) detonators, packaged emulsion gel as the bottom charge load, and 0.8 g/cc ANFO as the column charge load. The drill hole geometry and blasting pattern of the case study mine is shown in Figure 3. Thurley established that Wipfrag is a picture examination framework for

evaluating the particle size distribution of materials [11]. WipFrag estimates a 2-D net and reproduces a 3-D dispersion utilizing the standard of Geometric likelihood [35-35]. WipFrag is described as a state-of-the-art image-based gravimetry framework primarily for black and white (gray tone) images, although it can also accept colored prints [11]. The images were analyzed with WipFrag® software to determine the fragmentation particle size, as shown in Figure 4. Representative samples were collected from the rock mass at each bench level blasted for the uniaxial compressive strength test. The samples were subjected to a strength test in accordance with the international society of rock mechanics ISRM, [37] and the strength of the rock samples were correlated with the blast fragmentation and explosive usage for the blast result performance selection for the model development. The Rock formation with close homogenous strength property was considered for model development in this study.

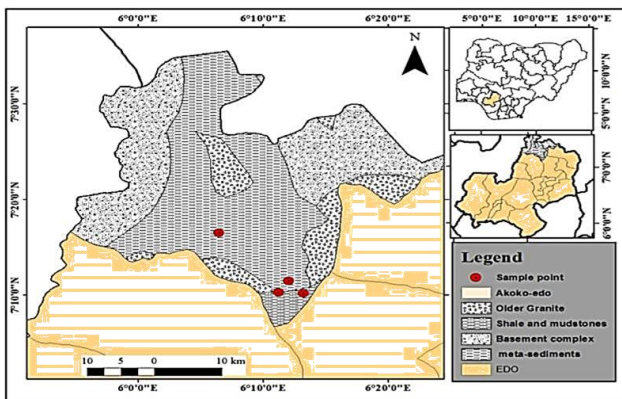


Figure 1. The geological map of Akoko Edo shows the study sample locations.

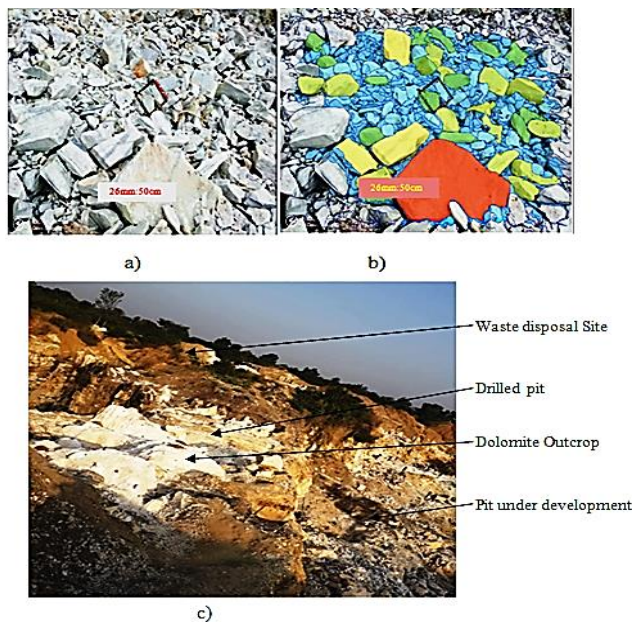


Figure 2. The Golden Girl quarry in-situ formation before and after blasting; a) The blasted rock mass with 1m by 1m scaling frame, b) The delineated image, and c. The mine face.

Da Gama proposed a microcomputer simulation model and a Comminution Theory model for predicting blast results using selected parameters [22-23]. Babaeian et al. [24] identified the main disadvantage of the model as the fact that the effect of stemming length, spacing, and bench height was ignored, as well as the absence of non-uniformity and uniformity prediction factors. Larsson et al. and Kuznetsov's models were introduced in the 1970s as predicting formulas

to improve blasting efficiency by predicting possible fragmentation results from specific combinations of blast parameters [25-26]. The models took into account factors, such as explosive type, rock mass classification, the impact of applied blast energy, and the evaluation of fragmentation uniformity and non-uniformity. The models' prediction performance was criticized due to their poor performance in predicting particle size distribution [24]. In 1983, the emergence of the Kuz-Ram model by Cunningham [27] came to the industry phase as a way to improve blasting work and cover up for previous models with limitations in applicability and efficiency. limitations. The model proposed an empirical equation (Eq. 1) for predicting the 50% passing size of a blasting round, considering both controllable and uncontrollable parameters that influence the rock fragmentation result. The first version of the model was further improved by Cunningham through the adoption of the Lilly blastability index to properly assess the model's performance and account for rock site condition and specification [27-30].

3.3. Development of Models

The obtained fragmentation analysis results and selected blast design parameters were used to develop the models for predicting the blast X_{50} and X_{80} particle sizes. The database's statistical range of the blast parameters and WipFrag analysis results obtained from the monitored blasts at the case study quarry is presented in Table 1. The Hunter-Point ANN (HP-ANN), SVM, Ridge regression, and MLR were used to develop models to estimate the X_{50} and X_{80} . For the two proposed models, thirty-five datasets were used with five input variables. The reason for smaller sample points (35) to predict the fragmentation size distribution is that most blasting operations in small hole mines are not consistent in parameters for some blast samples. However, the datasets used in both cases are enough to make reasonable soft computing models, as many authors have used an equal or lesser number of datasets to develop acceptable models. For instance, Bahrami et al. [16] used thirty-four datasets to predict the fragmentation size of the rock, 20 datasets were used by Gokceoglu and Zorlu [38] to predict the blast-induced ground vibration, Muhammed et al. [39] used 30 datasets to estimate organic and inorganic constituents in coal, and Lee et al. [40] used 30 datasets to predict the rock properties.

Figure 5 presents the correlation matrix, which shows the relationship between the input and output variables. The correlation matrix shows the sensitivity of all the input parameters to the dependent variable. The following observations were drawn from the sensitivity analysis; X_{50} and X_{80} have a highly negative correlation with the powder factor, and a slightly positive correlation with B/S, Stiffness Ratio, and D/B. This means that as the stemming, stiffness ratio, and B/S increase, the X_{50} increases, and as the powder factor decreases, the X_{50} and X_{80} increase. Many of the independent variables are highly correlated (both positively and negatively). Thus, while building the model, we will have to pay attention to multicollinearity.

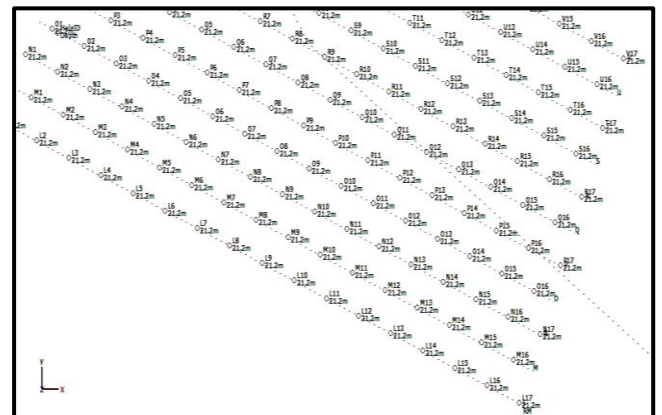


Figure 3. Mine's blast parameter design.

Figure 6a shows the relationship between rock strength and the powder factor used in the experiment blasting. The results revealed that a high-strength rock mass requires more explosive powder. In the case study mine, the maximum powder factor used was 0.98Kg/m³. The fragmentation size was also compared to the rock strength, as shown in Figure 6b. The results show that high-strength rock produces larger fragmentation sizes during some blast rounds. As mentioned by Villeneuve et al., a few blasts have no response to strength properties due to water, blast design property variation, and differences in rock characteristics [41].

Table 1. Blast and rock property data Visualization.

Parameters	Min.	Max.	Mean	Standard Deviation
Stemming (m)	0.2796	1.2	0.8198	0.3565
Burden (m)	0.6818	0.9231	0.8012	0.0712
Stiffness	1.0667	1.8571	1.6143	0.1942
Spacing (m)	0.7	1.3	1.047	0.1131
De/B	0.0333	0.0571	0.0486	0.0057
(kg/m ³)	0.4374	0.973	0.8058	0.1339
UCS (MPa)	167.75	186.25	172	5.5134
X50 (%)	0.1155	0.8018	0.3686	0.1578
X80 (%)	0.3715	1.1729	0.6661	0.196

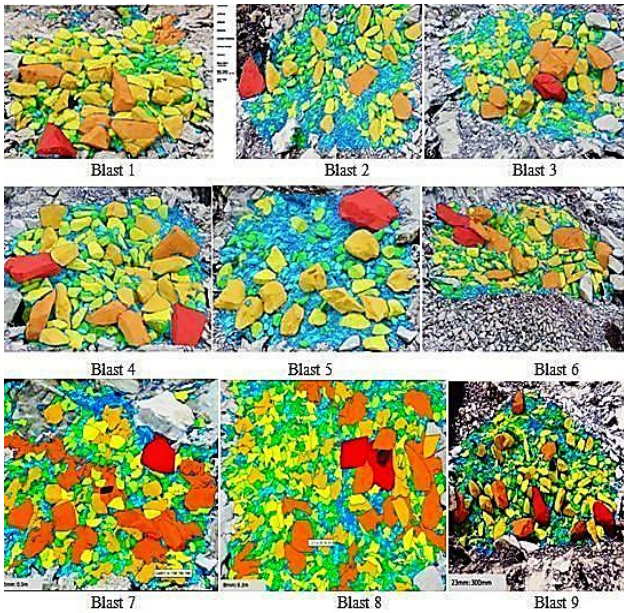


Figure 4. Blast image analysis result for nine blasts round using WipFrag software.

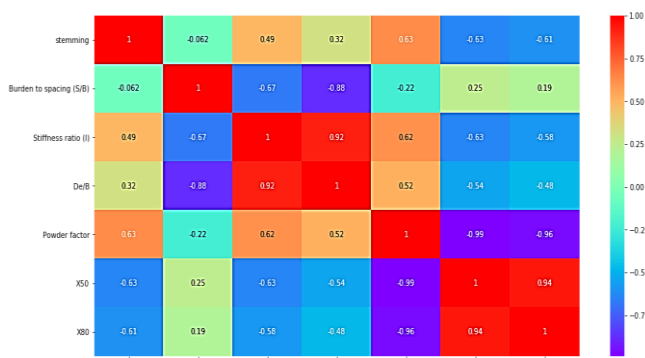


Figure 5. Correlation matrix showing the relationship between the input and output variables.

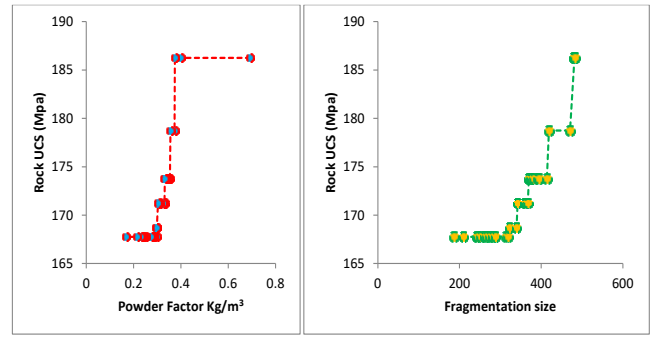


Figure 6. Relationship between the dolomite rock strength, (a) powder factor, and (b) fragmentation size.

3.3.1. Hunter Point-ANN (HPANN) approach to predict blast fragmentation

The application of the ANN modelling approach in engineering and scientific problems has grown significantly over the previous year [13]. ANN is a computational modelling technique that mimics the structure and functions of natural neural networks. These networks are highly functional in fitting non-linear and perceiving patterns [42]. The pattern of the variables is modeled by artificial neurons based on preceding learning algorithms. During the model training process, associated weights are assigned to the interconnections between the ANN layers which are adjusted through the transfer function as the training progresses [39]. The artificial neural technique adopted in this research is trained using a backpropagation algorithm. Abiodun et al. established that the feed-forward BPNN comprises three layers which are: the input layer, the hidden layer, and the output layer [13].

The Hunt Point ANN training process involves optimizing the training algorithm several times alongside neuron adjustment. This approach was done using the back propagation training algorithm with both Bayesian Regularization and Levenberg-Marquardt (LM) training algorithms. 80% of the datasets were used for training, while 10% each were used for validation and testing, respectively. Three different model architectures (5:3:1, 5:5:1, and 5:10:1) were checked with the hyperbolic tangent function as the transfer function used for the hidden and output layers in the three cases for each of the proposed ANN models. The 6-3-1 ANN architecture trained thrice using Bayesian Regularization with the sigmoid transfer function performed best for the X₅₀ and X₈₀ prediction as indicated by the coefficient of determination and RSME in Table 2. The input and output parameters used in developing ANN models are presented in Table 1. Thirty-five datasets were used to train the neural network in the MATLAB® environment using the MATLAB® nntstart toolbox. The input and output variables elements were normalized (scaled) between -1 and 1 using Eq. (2) to achieve dimensional consistency in the variable elements and also to eliminate over-fitting.

$$X_i = \frac{2(Y_i - Y_{min})}{(Y_{max} - Y_{min})} - 1 \tag{2}$$

Where X_i is the scaled element, Y_i is the actual data to be scaled; Y_{max} and Y_{min} are the maximum and minimum values of the actual data, respectively. Five datasets have been used for testing and validation of neural networks. The connection structure of the ANN and its performance during training are shown in Figure 7. The regression plots of ANN during training, testing, and validation indicate the excellence of the selected network, as shown in Figure 6c. The optimum model hyper parameters were de-normalized using Eq. (3)

$$Y_i = \left(\frac{Y_{max} - Y_{min}}{2}\right) X_p + \left(\frac{Y_{max} + Y_{min}}{2}\right) \tag{3}$$

Where X_p is the predicted element Y_i is the actual predicted data de-normalized; Y_{max} and Y_{min} are the maximum and minimum values of the actual data, respectively.

The optimum model with architecture 5-3-1 was transformed into the

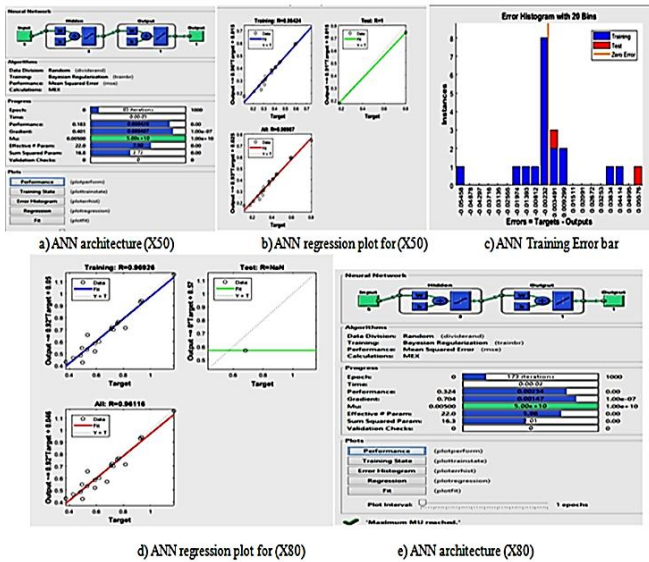


Figure 7. The ANN model Training output for Mean size (X_{50}).

mathematical expression using Eq. (4) which shows the general form of the operating principle of the ANN model, as noted by Lawal et al. [43].

$$P_j = f_{sig} / p_{urlin} [b_0 + \sum_{k=1}^n [f_{sig}(b_{nk} + \sum_{i=1}^m w_{ik} \Gamma_i^{w_{ik}})]] \quad (4)$$

where n is the number of neurons in the hidden layer; b_{nk} is the bias in the k th neuron of the hidden layer; b_0 is the bias in the output layer; w_{ik} is the weight of the connection between the k th of the hidden layer and the single output neuron; w_{ik} is the weight of the connection between the

i th input parameter and the hidden layer; Γ_i is the input variable i ; p_j is the output variable; f_{purlin} and f_{sig} are the linear and nonlinear transfer functions, respectively.

The ANN mathematical expression for X_{50} is presented in Eq. (5) and the expression for X_{80} is presented in Eq. (6).

$$X_{50} = 0.1292 \tanh(b_1 + b_2 + b_3 - 0.2219) + 0.1869 \quad (5)$$

$$b_1 = -0.7718 \tanh(-0.2590H/B - 0.3078D/B - 0.13443T + 0.2063 B/S + 0.7732K + 2.8369)$$

$$b_2 = -0.5468 \tanh(0.1803H/B + 0.1534D/B - 0.09932T - 0.1468 B/S + 0.3651 K + 0.0258)$$

$$b_3 = -0.4464 \tanh(-0.1621H/B - 0.0423D/B + 0.0633T + 0.3661B/S - 0.5682K - 0.01721)$$

$$X_{80} = 0.2222 \tanh(b_1 + b_2 + b_3 + 0.0401) + 0.40795 \quad (6)$$

$$b_1 = -0.6633 \tanh(-0.0142H/B + 0.0457D/B + 0.00022T - 0.0094B/S - 0.6121K + 0.0238)$$

$$b_2 = 0.4622 \tanh(-0.0375H/B + 0.0095D/B - 0.04027T + 0.0075B/S - 0.4249K + 0.02087)$$

$$b_3 = -0.6561 \tanh(0.0174 H/B - 0.0424 D/B + 0.00346T + 0.0069 B/S + 0.609K - 0.0231)$$

Where X_{50} and X_{80} are the 50% and 80% passing size in mm, respectively, T is the stemming length in m, B is the burden in m, H is the drill hole length in m, S is the spacing in m, D is the drill hole diameter in m, K is the powder factor in Kg/ton, b_1 , b_2 , b_3 are the total layer weight effect.

The two algorithms considered performed closely well with low prediction error for both the training and testing datasets. The training process also revealed that the Bayesian Regularization algorithm had a slower training time compared to the LM algorithm. The low-range RSME value of the two models shows a good prediction result, with the Bayesian Regularization algorithm being the best-fitting model for both the X_{50} and X_{80} datasets.

The developed neural network models are suitable for practical use at the mine with an R2 value of 0.812 for X_{80} and 0.943 for X_{50} . The ANN model has shown a good performance in the prediction of fragmentation size, as shown in this study and other research, such as Kulatilake et al. [44].

Table 2. The model Performance for two Different ANN Algorithms.

Outputs	Models	Bayesian Regularization Algorithm		Levenberg-Marquardt Algorithm	
		R ²	RSME	R ²	RSME
X_{80}	5:3:1	0.9409	0.00233	0.923521	0.00267
	5:5:1	0.9216	0.00263	0.859329	0.0137
	5:10:1	0.923521	0.00288	0.935089	0.00247
X_{50}	5:3:1	0.982081	0.000399	0.1369	0.0339
	5:5:1	0.982081	0.000411	0.942841	0.000171
	5:10:1	0.976144	0.00054	0.9604	0.00083

3.3.2. Multi-variant regression analysis (MVRA)

The network relation between the variables can also be calculated using multi-variant regression analysis (MVRA) Eq. (7) is used to develop a multivariate linear regression equation for the prediction of X_{50} and X_{80} .

$$Y(X) = \beta_0 + \beta_1 x_1 + \beta_2 x_2 + \dots + \beta_n x_n \quad (7)$$

Where, $\beta_1, \beta_2, \dots, \beta_n$, are the coefficients of the regression model, β_0 is the intercept, $Y(x)$ is the predictive value, and x_1, x_2, \dots, x_n are the independent variables.

Eqs. (8-9) were generated for X_{80} and X_{50} prediction using SPSS®. MVRA was conducted with the same datasets and the same input parameters used in ANN.

$$X_{80} = 0.013D/B - 0.846H/B - 0.534T - 0.0103B/S - 1.568K + 4.120 \quad (8)$$

$$X_{50} = -0.001D/B + 0.012 H/B - 0.581T + 0.818 B/S - 1.173K + 1.312 \quad (9)$$

Where, X_{50} and X_{80} are the 50% and 80% passing sizes in mm, respectively, T is the stemming length in m, B is the burden in m, H is the drill hole length in m, S is the spacing in m, D is the drill hole diameter in m, and K is the powder factor in Kg/ton.

3.3.3. Support Vector Machine (SVM)

Support Vector Machine, according to Reddy, is considered to be the most widely used machine learning module in the field of geotechnical engineering and tunneling [45]. SVM utilizes an optimization scheme to minimize an objective cost function, especially an ϵ -insensitive loss function, which is comprised of nonlinear kernel function sets (which can transform the input data from a lower dimensional to a higher-dimensional feature space, a procedure commonly known as mapping). SVM can approximate the correlations between the inputs and outputs in a dataset in an inherent, nonlinear fashion. The linear function of SVM is expressed in Eq. (10).

$$F(a) = w \times a + d \quad (10)$$

Where a is the input variable, w is the weight vector, and d indicates the model error values.

The SVM data training process is characterized by four main kernel functions, including the sigmoid function, linear, polynomial, and radial base (RBF) function [46]. The RBF kernel has been proven to have the ability to perform normally on a variety of databases [46]. In this study, the RBF kernel function with a kernel (γ) operating parameter set to 0.01 and a coefficient of penalty (C) set at 10 was considered the best. For the adopted RBF kernel function in this study, Eq. (10) was transformed into Eqs. (11-12). The result of the SVM model is presented in Figure 8.

$$f(a) = w \times H(a, ai) + d \quad (11)$$

$$H(a, ai) = \exp \frac{|a-ai|^2}{2\sigma^2} \quad (12)$$

Where; $H(a, ai)$ is the kernel function, and σ variance and our hyper parameter.

3.3.4. Ridge Regression Analysis

The ridge regression is a type of regressor used in modelling datasets. The proposed prediction model was developed by modifying ordinary least squares regression in a way that is helpful to avoid overfitting in predictions. In Ordinary Least Squares, the weight estimator is computed using Eq. (13). For better modelling results, this study adopted Eq. (14) in the ridge regression.

$$\beta = (X^T X)^{-1} X^T y \quad (13)$$

$$\beta = (X^T X + \lambda I)^{-1} X^T y \quad (14)$$

Where I is the identity matrix, and λ is a new input variable introduced into the model. In the ridge regression, λ is controlled by a hyper parameter, and $\hat{\alpha}$ is the expression for the decision factor (DF) in Eq. (18) was developed to provide further evaluation of the performance of the developed models based on the combination of the three adopted indices. The higher the value of the decision factor (DF) the more accurate the proposed model. the parameter that controls the over-fitting penalty.

To develop the proposed predictive model for X_{50} and X_{80} using ridge regression, a user-coding approach on Python[®] was used. The modelling was conducted with the same datasets and input parameters as those used for ANN training. Different values were set for $\hat{\alpha}$ with 1 giving the optimum value for both the training and testing data. Figure 9 shows the performance of the developed regression model.

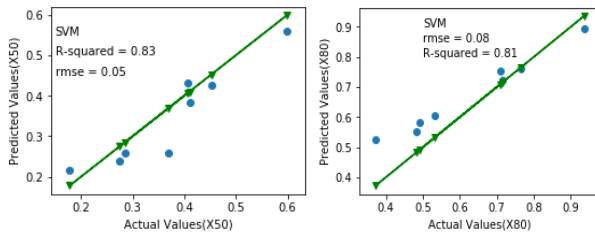


Figure 8. Graph showing the SVM regression performance for the developed models.

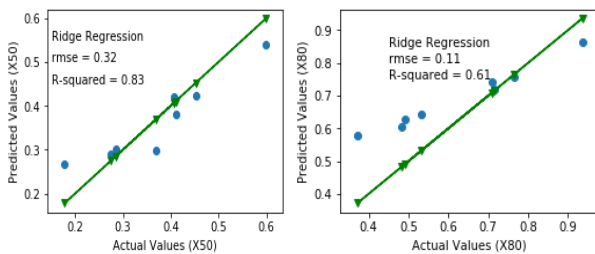


Figure 9. Graph showing the Ridge regression performance for the developed models.

4. Results and Discussion

4.1. Model Relationship

Four proposed models were developed with HP-ANN, MVR, SVM, and Ridge regression for the prediction of dolomite blast fragmentation size (X_{50} and X_{80}). The trained and optimized models were validated by ten datasets to determine the best model for fragmentation size prediction. The validation results are shown in Fig.10, with HP-ANN, MVR, SVM, and Ridge regression having R^2 values of 0.812, 0.673, 0.661, and 0.659, respectively for X_{80} prediction. The high R^2 value of HP-ANN makes it more suitable for the prediction of blast fragmentation

compare to the other three models with a lower coefficient of determination.

The predicting performance of the four proposed models was determined utilizing three well-known statistical differences and efficiency indicator indices, as shown in Eqs. (15-17). Root means square deviation (RMSD) and man bias (MB) were used as statistical difference indicators to evaluate the significant difference between the measured fragment size obtained from Wipfrag and the predicted sizes by each proposed model. Also, the Nash-Sutcliffe index for the coefficient of efficiency determination was used to evaluate the model prediction efficiency in percentage [48].

$$RMSD = \sqrt{\frac{\sum_{i=1}^N (F_i - M_i)^2}{N}} \quad (15)$$

$$MB = \frac{1}{N} \sum_{i=1}^N (F_i - M_i) \quad (16)$$

$$NS = 1 - \frac{\sum_{i=1}^N (M_i - F_i)^2}{\sum_{i=1}^N (M_i - M_e)^2} \quad (17)$$

Where N indicates the number of datasets, M is the measured value, F denotes the model predicted value, and M_e is the mean value of the measured value, respectively.

$$DF = NS - RMSE + MB \quad (18)$$

Where NS is the Nash-Sutcliffe index in percentage, $RMSD$ is the root mean square error, and MB is the mean bias. The model performance validation result is presented in Figures 10 and 11. The closer the Nash-Sutcliffe novel index is to 100, the higher the efficiency of the proposed model, and the closer calculated value of $RMSE$ and MB , the best the model performance [48]. Therefore, HP-ANN gives the highest value of NS , R^2 , DF , and the lowest value of $RMSE$, and MB , which makes it the most suitable model for the prediction of dolomite quarry fragmentation size distribution. The low value of MB for HP-ANN (Table 3) shows that it underestimates the predicted blast fragment size, while the high MB value for SVM, R_i , and MVR shows that it is overestimating the measured fragmentation size, as shown in Fig. 10. The both comparison charts, the indices of the model performance, and the decision factor, all indicate that the Hunter point ANN models give excellent predictions for the fragmentation 80% and 50% passing size of blast fragmentation in the dolomite quarry.

5. Conclusion

In this study, a new predictive model based on ANN was developed for estimating blast particle size distribution at small-scale mines, and the results were compared to those of SVM, Ridge, and Multivariate (MVR) regression models. The developed model with the new data set, hunter-Point artificial neural network (HP-ANN), with a 5:3:1 architecture, trained by the Bayesian Regularization algorithm three times with a sigmoid transfer function, has the highest prediction accuracy. The coefficient of correlation, root means square deviation (RMSD), Nash-Sutcliffe index (NS), and mean bias (MB) were used to assess the performance of the models used.

The key results of this study are summarized as follows:

1. The study revealed that rock strength influences blast fragmentation results. Based on the rock strength properties, the fragmentation size increases with an increase in rock strength.
2. The result of the statistical indicator indices ($RMSE$, MB , NS , R^2) used for the evaluation of the proposed models showed that the HP-ANN has the highest predictive accuracy. The values of $RMSE$, MB , NS , and R^2 for X_{50} are 0.027, 0.17, 88.07%, and 0.94, respectively, and for X_{80} they are 0.051, 0.23, 76.26%, and 0.81, respectively.
3. The MVR model possesses predictive accuracy lesser than HP-ANN, but higher than SVM and Ridge regression models.
4. A new model evaluator was developed called the decision factor. Its application indicates the HP-ANN model is the best model suitable for the prediction of blast fragment size distribution in a dolomite quarry.

The proposed model's limitation to small-hole drill dolomite quarry is a drawback, but further work, including a larger dataset from other types of aggregate quarries, is recommended to broaden the proposed model's application scope. Furthermore, the authors intend to investigate fragmentation size distribution using hybrid and ensemble learning, as well as other optimization-based machine learning approaches. Furthermore, some other influential attributes will be added to the blasting dataset to improve the accuracy of the fragmentation size distribution prediction.

Acknowledgments

The blasting images in this research were analyzed using Wipfrag software with the assistance of Engineer Barry McCreddie, Drilling and Blasting Operational Engineer MBM in Blast Ltd. Company N0:09198751/ 2 Halliwell Court, Elworth, Sandbach, CW11 3AQ, England. Email: barry@minblast.co.uk mobile: +447596455438, your assistance is acknowledged. The authors also acknowledge Taiwo Tosin Mojisola for her numerable support during the revision of this manuscript.

Table 3. Performance evaluation of each developed model for the blast fragment size prediction.

	RSMD		MB		NS (%)		R ²		DF	
	X50	X80	X50	X80	X50	X80	X50	X80	X80	X50
Ri	0.0675	0.11	0.26	0.34	31.16	23.72	0.743	0.66	24.167	31.48
SVM	0.066	0.086	0.26	0.29	37.12	39.23	0.785	0.66	39.62	37.45
HP-ANN	0.027	0.051	0.17	0.23	88.07	76.26	0.943	0.81	76.54	88.26
MVR	0.028	0.060	0.168	0.25	87.24	67.37	0.795	0.67	67.67	87.44

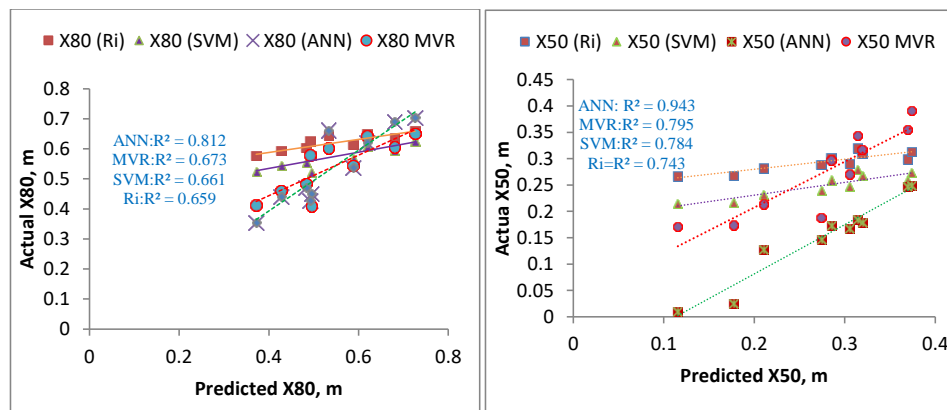


Figure 9. The model performance validation for fragment size prediction; a. validation for X₈₀ predictions, b. validation for X₅₀ predictions.

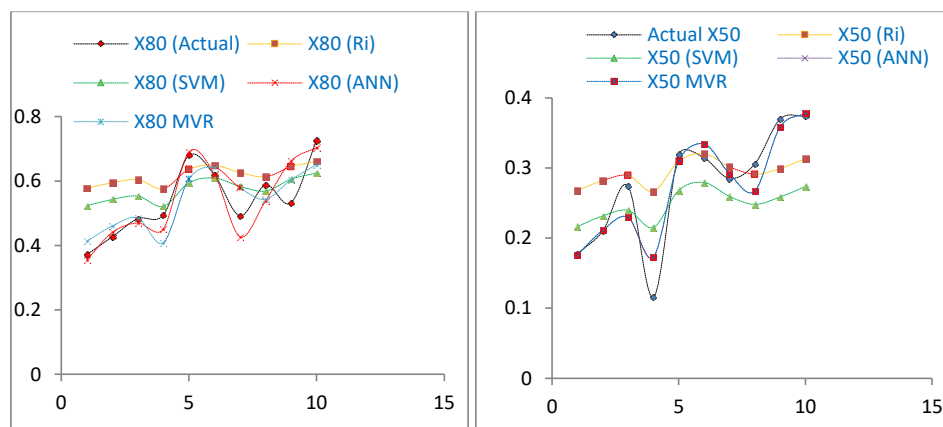


Figure 10. Evaluation and comparison of the four proposed models.

REFERENCES

- [1] Kansake, B. A., Temeng, V. A. And Afum, B. O. (2016). Comparative Analysis of Rock Fragmentation Models – A Case Study. 4th UMaT Biennial International Mining and Mineral Conference, 1–11.
- [2] Cardu, M., Seccatore, J., Vaudagna, A., Rezende, A., Galvão, F., Bettencourt, J., and Tomi, G. D. (2015). Evidences of the influence of the detonation sequence in rock fragmentation by blasting—Part I. Rem: Revista Escola de Minas, 68, 337–342.
- [3] Kanchibotla, S.S., Valery, W. and Morrell, S., (1998). Modelling fines in blast fragmentation and its impact on crushing and grinding. Proceedings of the. Explo 1999 Conference, Carlton, Victoria, Australian, 137–144.

- [4] Ouchterlony, F. (2005). The Swebrec function: linking fragmentation by blasting and crushing. *Mining Technology*, 114(1), 29-44.
- [5] Vamshidhar, K. and Venkatesh, H. S. (2010). Review of Models for Prediction of Rock Fragmentation due to Blasting, *Journal of the Explosives Safety And Technology Society (Visfotak) India: Dealing With Safety And Technological Aspects Of The Explosives Industry*, 5, 23-30.
- [6] Abuhasel, K.A. (2019). A comparative study of regression model and the adaptive neuro fuzzy conjecture systems for predicting energy consumption for jaw crusher. *Applied Sciences*, 9(18), 3916.
- [7] Taiwo, B. O. (2022). Effect of charge load proportion and blast controllable factor design on blast fragment size distribution. *Journal of Brilliant Engineering*, 3, 4658.
- [8] Tiile, R. N. (2016). Artificial neural network approach to predict blast-induced ground vibration, airblast and rock fragmentation. *Missouri University of Science and Technology*.
- [9] InanlooArabi Shad, H., Sereshki, F., Ataei, M. And Karamoozian, M. (2018). Investigation of the rock blast fragmentation based on the specific explosive energy and in-situ block size. *International Journal of Mining and Geo-Engineering*, 52(1), 1-6.
- [10] Al-Thyabat, S. and Miles, N. J. (2006). An improved estimation of size distribution from particle profile measurements. *Powder Technology*, 166(3), 152-160.
- [11] Thurley, M. J. (2011). Automated online measurement of limestone particle size distributions using 3D range data. *Journal of Process Control*, 21(2), 254-262.
- [12] TavakolElahi, A. and Hosseini, M. (2017). Analysis of blasted rocks fragmentation using digital image processing (case study: limestone quarry of Abyek Cement Company). *International Journal of Geo-Engineering*, 8(1), 1-11.
- [13] Abiodun, O. I., Jantan, A., Omolara, A. E., Dada, K. V., Mohamed, N. A., and Arshad, H. (2018). State-of-the-art in artificial neural network applications: A survey. *Heliyon*, 4(11), e00938.
- [14] Ghaeini Hesarouieh, N., Mousakhani, M., Bakhshandeh Amnieh, H., and Jafari, A. (2017). Prediction of fragmentation due to blasting using mutual information and rock engineering system; case study: Meydook copper mine. *International Journal of Mining and Geo-Engineering*, 51(1), 23-28.
- [15] Sereshki, F., Hoseini, S. M., and Ataei, M. (2016). Blast fragmentation analysis using image processing. *International Journal of Mining and Geo-Engineering*, 50(2), 211-218.
- [16] Bahrami, A., Monjezi, M., Goshtasbi, K., and Ghazvinian, A. (2011). Prediction of rock fragmentation due to blasting using artificial neural network. *Engineering with computers*, 27(2), 177-181.
- [17] Enayatollahi, I., Aghajani Bazzazi, A., and Asadi, A. (2014). Comparison between neural networks and multiple regression analysis to predict rock fragmentation in open-pit mines. *Rock mechanics and rock Engineering*, 47(2), 799-807.
- [18] Rezaei, M., Hossaini, M. F., Majdi, A., and Najmoddini, I. (2017). Determination of the height of distressed zone above the mined panel: An ANN model. *International Journal of Mining and Geo-Engineering*, 51(1), 1-7.
- [19] Sayadi, A., Monjezi, M., Talebi, N., and Khandelwal, M. (2013). A comparative study on the application of various artificial neural networks to simultaneous prediction of rock fragmentation and backbreak. *Journal of Rock Mechanics and Geotechnical Engineering*, 5(4), 318-324.
- [20] Amoako, R., Jha, A., and Zhong, S. (2022). Rock fragmentation prediction using an artificial neural network and support vector regression hybrid approach. *Mining*, 2(2), 233-247.
- [21] Kanchibotla, S.S., Valery, W. and Morrell, S., (1998). Modelling fines in blast fragmentation and its impact on crushing and grinding. *Proceedings of the Explo 1999 Conference*, Carlton, Victoria, Australian, 137-144.
- [22] Da Gamma, C.D. (1984). Microcomputer simulation of rock blasting to predict fragmentation, *Proceedings of the 25th U.S. Symposium on Rock Mechanics*, Evanston, Illinois, pp. 1018-1030.
- [23] Da Gamma, C.D. (1983). Use of Comminution Theory to Predict Fragmentation of Jointed Rock Masses Subjected to Blasting. In: *Proceedings of the First International Symposium on Rock Fragmentation by Blasting*, Lulea, Sweden, pp. 565-579.
- [24] Babaeian, M., Ataei, M., Sereshki, F., Sotoudeh, F. and Mohammadi, S. (2019). A new framework for evaluation of rock fragmentation in open pit mines. *Journal of Rock Mechanics and Geotechnical Engineering*, 11(2), pp. 325-336.
- [25] Kuznetsov, V.N. (1973). The Mean Diameter of the Fragments Formed by Blasting of Rock. *Soviet Mining Sci. Part 2*, pp. 39-43.
- [26] Larsson, B., Hemgren, W., and Brohn, C.E. (1973). *Styckefallsutredning*. Skanska, Cement gjuteriet.
- [27] Cunningham, C.V.B. (2005). The Kuz-Ram fragmentation model-20 years on, *Proceedings of the 3rd European Federation of Explosives Engineers World Conference on Explosives and Blasting*, Brighton. 4, pp. 201-210.
- [28] Cunningham, C.V.B. (1983). The Kuz-Ram model for prediction of fragmentation from blasting. In: *Proceedings of the 1st international symposium on rock fragmentation by blasting*. Sweden: Luleå University of Technology. P. 439-453.
- [29] Lilly, P.A. (1986). An empirical method of assessing rock mass blastability. In: *Proceedings of the large open pit mine conference*. Carlton, Australia: AusIMM. pp. 89-92.
- [30] Cunningham, C.V.B. (1987). Fragmentation estimations and the Kuz-Ram model e four years on. In: *Proceedings of the 2nd international symposium on rock fragmentation by blasting*. p. 475-487.
- [31] Ouchterlony, F. and Sanchidrián, J.A. 2019. A review of development of better prediction equations for blast fragmentation. *Journal of Rock Mechanics and Geotechnical Engineering*, vol. 11, no. 5. pp. 1094-1109.
- [32] Singhai, M. P. and Pyasi, A. (2022). Application of anfis model in explosives. *International Research Journal of Modernization in Engineering Technology and Science*, 4(2), 394-398. www.irjmets.com.
- [33] Dhekne, P. Y., Pradhan, M., Jade, R. K., and Mishra, R. (2017). Boulder prediction in rock blasting using artificial neural network. *ARP Journal of Engineering and Applied Sciences*, 12(1), 47-61.
- [34] Zangoei, A., Monjezi, M., Armaghani, D.J., Mehrdanesh, A., and Ahmadian, S. (2022). Prediction and optimization of flyrock and oversize boulder induced by mine blasting using artificial intelligence techniques. *Environmental Earth Sciences*, 81(13), 1-13.

- [35] Tavakol Elahi, A. and Hosseini, M. (2017). Analysis of blasted rocks fragmentation using digital image processing (case study: limestone quarry of Abyek Cement Company). *International Journal of Geo-Engineering*, 8(1), 1-11.
- [36] Yang, Z., He, B., Liu, Y., Wang, D., and Zhu, G. (2021). Classification of rock fragments produced by tunnel boring machine using convolutional neural networks. *Automation in Construction*, 125, 103612.
- [37] ISRM. (1989), Suggested Methods for the Quantitative Description of Uniaxial Compressive Strength Test and Discontinuities in Rock Masses. In: Brown ET editor. *Rock Characterization, Testing and Monitoring: ISRM Suggested Methods*. Oxford: Pergamon, 256-300.
- [38] Gokceoglu, C. and Zorlu, K. (2004). A fuzzy model to predict the uniaxial compressive strength and the modulus of elasticity of a problematic rock. *Eng Applied Artificial Intelligence*, 17:61-72.
- [39] Muhammed, N. S., Haq, M. B., Al-Shehri, D., Rahaman, M. M., Keshavarz, A., and Hossain, S. Z. (2020). Comparative study of green and synthetic polymers for enhanced oil recovery. *Polymers*, 12(10), 2429.
- [40] Lee, J. M., Yoo, C. and Lee, I. B. (2004). Statistical process monitoring with independent component analysis. *Journal of process control*, 14(5), 467-485.
- [41] Villeneuve, M. C., Diederichs, M. S., and Kaiser, P. K. (2012). Effects of grain scale heterogeneity on rock strength and the chipping process. *International Journal of Geomechanics*, 12(6), 632-647.
- [42] Jong, Y.H. and Lee, C.I. (2004). Influence of geological conditions on the powder factor for tunnel blasting. *Int J Rock Mechanics and Mining*, 41, 533-538.
- [43] Lawal, A.I., Aladejare, A.E., Onifade, M., Bada, S. and Idris, M.A. (2021). Predictions of elemental composition of coal and biomass from their proximate analyses using ANFIS, ANN and MLR. *International Journal of Coal Science and Technology*, 8(1), 124-140. <https://doi.org/10.1007/s40789-020-00346-9>
- [44] Kulatilake, P. H. S. W., Qiong, W., Hudaverdi, T., & Kuzu, C. (2010). Mean particle size prediction in rock blast fragmentation using neural networks. *Engineering Geology*, 114(3-4), 298-311.
- [45] Reddy, Y. R. (2019). A Machine Learning Framework For Predicting Displacements Due To Deep Excavations And Tunnels. *International Journal of Creative Research Thoughts (IJCRT)*, ISSN, 2320-2882.
- [46] Hong, H., Pradhan, B., Bui, D. T., Xu, C., Youssef, A. M., and Chen, W. (2017). Comparison of four kernel functions used in support vector machines for landslide susceptibility mapping: a case study at Suichuan area (China). *Geomatics, Natural Hazards and Risk*, 8(2), 544-569.
- [47] Amami, R., and Smiti, A. (2017). An incremental method combining density clustering and support vector machines for voice pathology detection. *Computers and Electrical Engineering*, 57, 257-265.
- [48] Coffey, M. E., Workman, S. R., Taraba, J. L., and Fogle, A. W. (2004). Statistical procedures for evaluating daily and monthly hydrologic model predictions. *Transactions of the ASAE*, 47(1), 59.